Improving Reliability of Particle Filter-Based Localization in Wireless Sensor Networks via Hybrid Particle/FIR Filtering

Jung Min Pak, Choon Ki Ahn, *Senior Member, IEEE*, Yuriy S. Shmaliy, *Fellow, IEEE*, and Myo Taeg Lim, *Member, IEEE*

***Abstract*—The need for accurate, fast, and reliable indoor localization using wireless sensor networks (WSNs) has recently grown in diverse areas of industry. Accurate localization in cluttered and noisy environments is commonly provided by means of a mathematical algorithm referred to as a state estimator or filter. The particle filter (PF), which is the most commonly used filter in localization, suffers from the sample impoverishment problem under typical conditions of real-time localization based on WSNs. This paper proposes a novel hybrid particle/finite impulse response (FIR) filtering algorithm for improving reliability of PF-based localization schemes under harsh conditions causing sample impoverishment. The hybrid particle/FIR filter detects the PF failures and recovers the failed PF by resetting the PF using the output of an auxiliary FIR filter. Combining the regularized particle filter (RPF) and the extended unbiased FIR (EFIR) filter, the hybrid RP/EFIR filter is constructed in this paper. Through simulations, the hybrid RP/EFIR filter demonstrates its improved reliability and ability to recover the RPF from failures.**

***Index Terms*—Hybrid particle/finite impulse response (FIR) filter, hybrid regularized particle/extended unbiased finite impulse response (RP/EFIR) filter, indoor localization, wireless sensor network (WSN).**

I. Introduction

INDOOR localization systems [1]–[8], which utilize informative facilities of wireless sensor network (WSN) technology, have been used for a variety of purposes, such as tracking workers and equipment in construction sites, vehicle tracking in parking lots, human localization in hospitals or intelligent buildings, cargo tracking systems in logistics, and robot tracking in museums or in factories [9]. Indoor localization systems typically take advantage of state estimators for accurate localization in cluttered and noisy indoor environments [1], [10], [11]. In particular, in order to overcome non-line-of-sight (NLOS) situations, accurate state estimation is essential [12]. The state estimator, also referred to as a stochastic filter, is a mathematical algorithm that can estimate state variables of a system from noisy measurements [13]. The best known is the Kalman filter (KF), which is optimal for linear systems with Gaussian noise [14]. For indoor localization problems, the state-space model is typically nonlinear; therefore, nonlinear filters such as the extended Kalman filter (EKF) and the particle filter (PF) are used [12], [15]. The PF, also referred to as Monte Carlo localization (MCL) [16]–[18], has gained wide currency in recent decades owing to its better performance in highly nonlinear environments [14] and its ability to solve a given global localization problem with no information about the initial position. Note that the EKF requires the initial position and can thus solve only local-localization (i.e., position tracking) problems [18].

Although the PF is algorithmically more transparent and simpler than the EKF, it has a serious drawback associated with loss of diversity among the samples resulting in failures of state estimation and large estimation errors (i.e., the PF failure) [14], [18], [19]. An associated problem, called sample impoverishment, usually occurs when the process/measurement noise is small or when the number of particles is insufficient. Several improved techniques, such as the regularized particle filter (RPF) [20], Markov chain Monte Carlo (MCMC) move step [21], combined PF/KF [22], and mixture MCL [16] have been proposed for overcoming the sample impoverishment problem by mitigating the loss of sample diversity. However, the improved PF techniques cannot completely prevent sample impoverishment. It is known that the improved PFs also can exhibit degraded performance or failures under severe conditions (e.g., very small process/measurement noise or a very small number of particles) [16], [18], [19]. Thus, a hedge against failures occurred in the improved PFs is necessary. To date, there have been various preventative methods against sample impoverishment and PF failures. However, an effective and general remedy to cure a completely failed (or diverging) PF has yet to be proposed.

Manuscript received October 30, 2014; accepted June 30, 2015. Date of publication July 29, 2015; date of current version October 02, 2015. The work of J. M. Pak and M. T. Lim was supported by the General Research Program through the National Research Foundation of Korea (NRF), funded by the Ministry of Education under Grant NRF-2013R1A1A2008698. The work of C. K. Ahn was supported in part by NRF, funded by the Ministry of Science, ICT, and Future Planning under Grant NRF-2014R1A1A1006101, and in part by the Human Resources Program in Energy Technology of the Korea Institute of Energy Technology Evaluation and Planning (KETEP) granted financial resource from the Ministry of Trade, Industry, and Energy, Republic of Korea, under Grant 20154030200610. The work of Y. S. Shmaliy was supported by the Royal Academy of Engineering under the Newton Research Collaboration Programme under Grant NRCP/1415/140. Paper no. TII-15-0815. *(Corresponding author: Choon Ki Ahn.)*

J. M. Pak, C. K. Ahn, and M. T. Lim are with the School of Electrical Engineering, Korea University, Seoul, 136-701, Korea (e-mail: destin11@korea.ac.kr; hironaka@korea.ac.kr; mlim@korea.ac.kr).

Y. S. Shmaliy is with the Department of Electronics Engineering, Universidad de Guanajuato, Salamanca 36885, Mexico (e-mail: shmaliy@ugto.mx).

Color versions of one or more of the figures in this paper are available online at http://ieeexplore.ieee.org.

Digital Object Identifier 10.1109/TII.2015.2462771

In recent years, real-time locating systems (RTLS) based on WSNs have attracted the attention of designers and users in industry. When applying a PF to an indoor RTLS for improving localization accuracy, the computational burden may become an issue. The RTLS requires fast computation for real-time processing, and the PF should use a small number of particles, which accelerates sample impoverishment. In addition, low measurement noises generated from accurate WSNs also cause sample impoverishment. Those requisite conditions in the RTLS are harsh for PF-based localization schemes to achieve reliable localization.

This paper proposes a novel hybrid particle/finite impulse response (FIR) filtering algorithm to improve reliability of PF-based localization under harsh conditions of RTLS based on WSNs. In the proposed hybrid filtering, a PF plays the role of a main filter, and a robust filter referred to as a FIR filter [1], [24]–[35] is used as an auxiliary filter. The main PF produces state estimates in normal situations in which sample impoverishment or failures do not occur. When the PF exhibits abnormally large estimation errors or divergent behaviors, the auxiliary FIR filter is operated for recovering the failed PF. The proposed hybrid filtering algorithm does not modify the PF algorithm; it only detects failures and recovers the PF. Thus, the hybrid filtering is applicable to any PF. In this paper, the RPF, which is well known and has been tested in diverse problems, is used to construct the hybrid filter. In addition, the extended unbiased FIR (EFIR) filter is adopted as the auxiliary FIR filter. The resulting filter, combining the RPF and the EFIR filter, is called the hybrid RP/EFIR filter. In localization problems using a mobile robot and WSNs, the hybrid RP/EFIR filter demonstrates its ability to recover from failures under harsh conditions of low measurement noise and a small number of particles. Statistical analysis verifies that the hybrid RP/EFIR filter improves reliability of localization compared to the pure RPF. In addition, the hybrid RP/EFIR filter is shown to be capable of solving the kidnapped robot problem and can reduce the computation time.

The contributions of this paper are as follows. The hybrid particle/FIR filtering is a novel algorithm for recovering a completely failed PF. To date, to the best of the present authors' knowledge, a general algorithm for recovering a completely failed PF has yet to be proposed. The sensor resetting technique proposed in [23] is available in very limited cases (e.g., visual object tracking) in which the samples of state can be directly drawn from the sensor readings. Since the hybrid particle/FIR filtering generates new samples using an auxiliary FIR filter, it can be used for general purposes. In addition, the hybrid particle/FIR filtering is a general algorithm that can adopt any PFs and nonlinear FIR filters. Combining a state-of-the-art PF with a nonlinear FIR filter, the hybrid filter can be upgraded to a new version. The hybrid particle/FIR filter overcomes limitations of both the PF and the FIR filter by utilizing the two filters jointly. The PF is a type of infinite impulse response (IIR) filters, and it exhibits better estimation accuracy than FIR filters under ideal (or normal) conditions. However, the PF may exhibit failures due to sample impoverishment, which can be caused by diverse factors. The FIR filter is a reliable filtering algorithm that is robust against modeling and computational errors; however, it exhibits inferior performance in normal situations to that of IIR-type filters. The hybrid particle/FIR filter behaves like a PF in normal situations and an FIR filter when PF failures occur. Therefore, the hybrid particle/FIR filter simultaneously achieves accuracy and reliability.

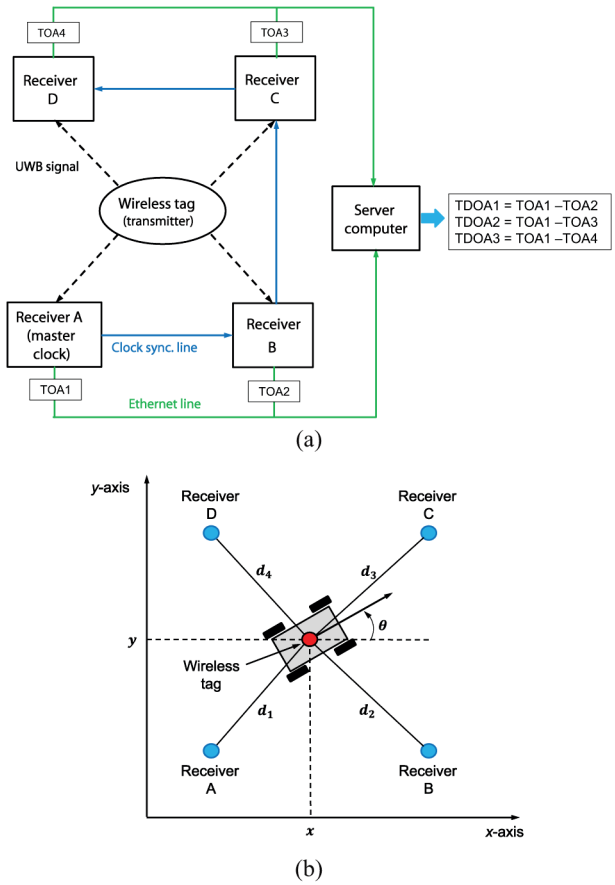

Fig. 1. Schematics of the mobile robot localization system. (a) Block-diagram of the WSN-based indoor localization system employing TDOA measurements. (b) 2-D schematic geometry.

This paper is organized as follows. In Section II, the PF-based robot localization scheme using a WSN is explained. In Section III, the hybrid particle/FIR filtering algorithm is proposed. In Section IV, simulation results under various harsh conditions are presented for demonstrating the effect and ability of the hybrid RP/EFIR filter. Finally, conclusion is drawn in Section V.

II. PF-Based Localization Scheme Using WSN for Mobile Robots

In this paper, an indoor localization system based on a WSN for tracking positions of mobile robots is considered. The indoor localization system consists of a wireless tag with a transmitter, four receivers, and a server computer. A 2-D schematic diagram of this system is shown in Fig. 1(a). A wireless tag attached to the mobile robot transmits a wireless signal. Four receivers installed at fixed positions with exactly known coordinates receive the wireless signal from the tag. The receiver's clocks are synchronized using the clock

synchronization line. The time-of-arrival (TOA) measurements are made, which give the traveling time of a wireless signal between the transmitter and each of the receivers. The TOA measurements are then transferred to a server computer to generate the time-difference-of-arrival (TDOA) measurements, which can be described by the following equation:

$$\begin{bmatrix} z_{1,k} \\ z_{2,k} \\ z_{3,k} \end{bmatrix} = \begin{bmatrix} h_{1,k} \\ h_{2,k} \\ h_{3,k} \end{bmatrix} = \frac{1}{c} \begin{bmatrix} d_1 - d_2 \\ d_1 - d_3 \\ d_1 - d_4 \end{bmatrix} \tag{1}$$

where $z_{1,k}$, $z_{2,k}$, and $z_{3,k}$ are the TDOA measurements (in units of nanoseconds) at discrete time index k; c is the speed of light [9], [15]. Here, d_i $(i = 1, 2, 3, 4)$ represents distances between the mobile robot and the receivers, as shown in Fig. 1(b), which is defined by the following equation:

$$d_i = \sqrt{(x_k - x_i)^2 + (y_k - y_i)^2} \tag{2}$$

where $(\mathbf{x}_k, y_k)$ are coordinates of the mobile robot location at time k, and (x_i, y_i) are fixed coordinates of the receivers.

At time index k, the mobile robot pose is described with the state vector $\mathbf{x}_k = [x_k \ y_k \ \theta_k]^T$, where x_k and y_k are the coordinates on a 2-D plane relative to an external coordinate frame, and θ_k is the heading angle [18]. Motion of the mobile robot is determined by the control commands $\mathbf{u}_k = [\Delta d_k \ \Delta\theta_k]^T$, where Δd_k is the incremental distance (in meters) and $\Delta\theta_k$ is the incremental change in heading angle (in degrees). The robot motion can be described by (3), (4), and (5) [1], [36]

$$x_k = f_{1,k} = x_{k-1} + \Delta d \cos\left(\theta_{k-1} + \frac{1}{2}\Delta\theta_k\right) \tag{3}$$

$$y_k = f_{2,k} = y_{k-1} + \Delta d \sin\left(\theta_{k-1} + \frac{1}{2}\Delta\theta_k\right) \tag{4}$$

$$\theta_k = f_{3,k} = \theta_{k-1} + \Delta\theta_k. \tag{5}$$

The localization accuracy is improved by equipping the mobile robot with a fiber optic gyroscope (FOG) [37] that directly measures the heading angle θ_k. Thus, the fourth measurement, defined by (6), is adopted

$$z_{4,k} = h_{4,k} = \theta_k \tag{6}$$

where $z_{4,k}$ is the measured θ_k. Combining all three TDOA measurements, defined by (1), with a measured heading angle, defined by (6), the measurement vector is constructed as $\mathbf{z}_k = [z_{1,k} \ z_{2,k} \ z_{1,k} \ z_{4,k}]^T$.

Now, the state equation and the measurement equation are defined as $\mathbf{f}_k = [f_{1,k} \ f_{2,k} \ f_{3,k}]^T$ and $\mathbf{h}_k = [h_{1,k} \ h_{2,k} \ h_{3,k} \ h_{4,k}]^T$, respectively. The following model can then represent the problem in state space:

$$\mathbf{x}_k = \mathbf{f}_k(\mathbf{x}_{k-1}, \mathbf{u}_k) + \mathbf{w}_k \tag{7}$$

$$\mathbf{z}_k = \mathbf{h}_k(\mathbf{x}_k) + \mathbf{v}_k \tag{8}$$

where the process noise $\mathbf{w}_k$ and the measurement noise $\mathbf{v}_k$ are zero-mean Gaussian with the covariances $\mathbf{Q}_k$ and $\mathbf{R}_k$, respectively. Given the state-space model (7) and (8), the mobile robot location and heading can be estimated using PF. Below, considering the PF-based localization algorithm, the drawbacks associated with fast (real-time) localization [14], [18], [19] are discussed, and then the problem is formulated.

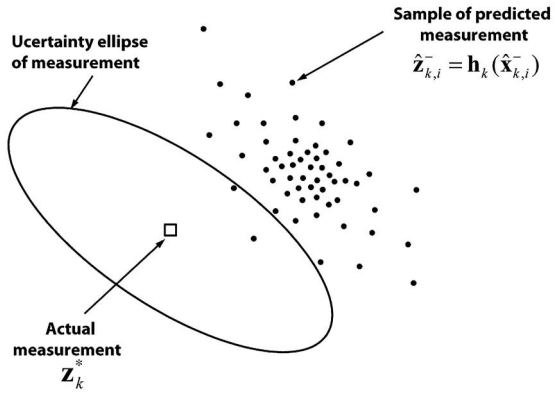

Fig. 2. Situation in which sample impoverishment occurs.

A. PF-Based Localization and Sample Impoverishment

The PF-based approach assumes that the robot coordinates are first-order Markov processes that evolve from one point to another with known initial and transition distributions. In turn, the conditionally independent observations depend only on the robot coordinates. In order to estimate x_k, y_k, and θ_k, PF generates at each time index k a set of samples that approximates the distributions of the coordinates conditioned on all past observations. This process is called *resampling* and it assumes that the particles with high weights (i.e., high likelihoods) will statistically be selected many times. This often leads to a loss of *diversity* among the particles, and the resultant particle set contains many repeated particles [19]. This problem is known as *sample impoverishment*, and it usually occurs when the process/measurement noise has low intensity or when the number of particles is small.

Fig. 2 gives a graphical illustration of a situation in which sample impoverishment occurs. In this figure, the dots represent samples of the predicted measurement $\hat{\mathbf{z}}_{k,i}^-$, which is defined as

$$\hat{\mathbf{z}}_{k,i}^- = \mathbf{h}_k(\hat{\mathbf{x}}_{k,i}^-) \quad (i = 1, 2, \ldots, N) \tag{9}$$

where $\mathbf{h}_k(\cdot)$ is the nonlinear function of the measurement equation, $\hat{\mathbf{x}}_{k,i}^-$ is the ith *a priori* particle (i.e., sample of the *a priori* estimated state), and N is the number of samples (i.e., the number of particles). In the Gaussian likelihood function, the likelihood (i.e., weight) of each particle is a reciprocal of the difference between the actual measurement and the predicted measurement. Thus, the closer the samples of predicted measurement $\hat{\mathbf{z}}_{k,i}^-$ are placed to the actual measurement $\mathbf{z}_k^*$, the higher the weight of the *a priori* particle. Observing Fig. 2, one notices that there are only two samples of predicted measurement located within the measurement *uncertainty ellipse* (also known as the *error ellipse*). Only two *a priori* particles $\hat{\mathbf{x}}_{k,i}^-$ can obtain significant weight, and resampling will repeat them multiple times as *a posteriori* particles $\hat{\mathbf{x}}_{k,i}^+$. This leads to sample impoverishment [14] and failures in PF-based robot localization. The above-described scenario is mostly due to low-intensity process/measurement noise and/or the small number of particles required for fast localization. Other factors may also cause sample impoverishment; therefore, much effort has been made by diverse authors to find a solution. Unfortunately, sample impoverishment is fundamental in PF

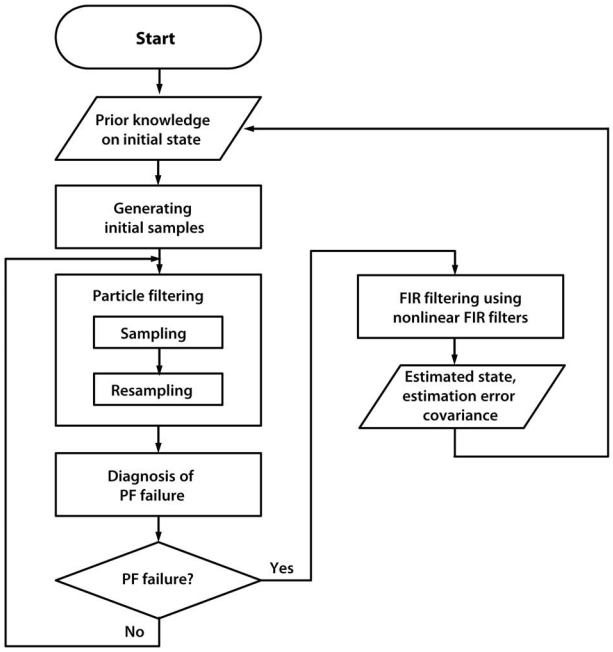

Fig. 3. Flowchart of hybrid particle/FIR filtering algorithm.

and cannot be avoided completely. Moreover, existing algorithms such as those in [20]–[22] are not able to recover the PF from failures.

III. Hybrid Particle/FIR Filtering

When a serious failure occurs in the PF algorithm, resetting the failed PF can be a good remedy. This approach involves two key processes; 1) detecting failures in the PF; and 2) generating new particles for the PF. First, to detect PF failures, a novel diagnosis algorithm based on the Mahalanobis distance is proposed in this paper. Second, to generate new particles for resetting PF, an auxiliary filter is utilized. The first requirement for the auxiliary filter is robustness. The auxiliary filter has to produce state estimates under the conditions in which the PF failure occurs. The auxiliary filter does not have to be very accurate, but it should be robust and stable. The second requirement for the auxiliary filter is that it can operate only occasionally, when necessary. This is necessary for reducing computational burden. If the PF and the auxiliary filter run simultaneously, excessive computational burden may become an issue. For fast computation and real-time processing, reducing computational burden is essential. The IIR-type filters, such as the EKF and the unscented Kalman filter (UKF), are not appropriate for the auxiliary filter, because they have a possibility of divergence. Moreover, the IIR-type filters require the prior estimate $\hat{\mathbf{x}}_{k-1}$ for producing the current estimate $\hat{\mathbf{x}}_k$. Thus, the IIR-type filters cannot realize the occasional execution. However, the FIR filters have built-in bounded-input bounded-output (BIBO) stability and special robustness against modeling and computational errors. In addition, the FIR filters can produce the current state estimate using recent finite measurements without the prior state estimate. In particular, the EFIR filter is one of the fastest FIR filters, because it has a Kalman-like form. Therefore, the EFIR filter is appropriate as the auxiliary filter.

Fig. 3 shows the flowchart of the proposed algorithm. The PF plays the role of the main filter that provides estimation of the mobile robot coordinates and heading in normal conditions. The PF is appropriate for the main filter, because it can provide better performance, when there is no failures, than nonlinear FIR filters. To use a nonlinear FIR filter as a main filter, the cumbersome problem of finding a suitable horizon size must be solved. A diagnosis of PF failures is conducted at every time. If the PF failure is detected, the auxiliary nonlinear FIR filter is operated to produce information for resetting the failed PF. In the following sections, the algorithm of hybrid particle/FIR filtering will be explained in detail.

A. Diagnosis of PF Failures

Wrong estimates at the PF output can be detected by taking into account the following features of sample impoverishment.

1) Only a few samples of predicted measurement falling within the measurement *uncertainty ellipse*.
2) The samples of the predicted measurement are far from the actual measurement.

Referring to the first feature, one can diagnose PF failures by checking the number of samples falling within the uncertainty ellipse. Classification methods using the uncertainty ellipse have been used in the area of multitarget tracking; this method is known as *ellipsoidal gating* [38]. The ellipsoidal gating for multitarget tracking is used for classification of the tracked positions of targets, whereas the proposed method is used to classify the predicted measurements. In order to recognize samples falling within the uncertainty ellipse, the *Mahalanobis distance* [39] and *chi-square distribution* [40] are used. The required chi-square value χ^2 is taken from a *chi-square table*. For example, the third-order system having three states requires $\chi^2 = 11.34$ for a confidence level of 99%. However, this

Algorithm 1. Diagnosis of PF Failure

Data: χ^2
Result: I_{failure}
begin
  - Compute the sample mean of the *a posteriori* particles at time k: $\mu_k = \frac{1}{N}\sum_{i=1}^{N} \hat{\mathbf{x}}_{k,i}^{+}$
  - Compute the predicted measurement of the sample mean: $\hat{\mathbf{z}}_{k,\mu} = \mathbf{h}_k(\mu_k)$
  - Compute the Mahalanobis distance $\mathcal{D}_k$ between the predicted measurement and the actual measurement:
  $\mathcal{D}_k = (\mathbf{z}_k^* - \hat{\mathbf{z}}_{k,\mu})\mathbf{R}_k^{-1}(\mathbf{z}_k^* - \hat{\mathbf{z}}_{k,\mu})$.
  if $\mathcal{D}_k > \chi^2$ **then**
    $I_{\text{failure}} = 1$ (the PF failure occurs).
    else
    $I_{\text{failure}} = 0$ (the PF failure does not occur).
  end if
end
† I_{failure} is a variable for indicating the PF failure.
† $\mathbf{R}_k$ is the covariance of the Gaussian measurement noise at time k.

method implies a large computational burden, because each sample undergoes testing. Thus, an alternative method that refers to the second feature of sample impoverishment is proposed. The *Mahalanobis distance* between the sample mean of predicted measurements and the actual measurement is computed. If the computed *Mahalanobis distance* is larger than the predetermined χ^2, it is judged that the PF failure occurs. This diagnostic procedure is summarized in Algorithm 1.

B. FIR Filtering Using Nonlinear FIR Filters

When the PF failure is detected by Algorithm 1, an auxiliary nonlinear FIR filter is operated. In this paper, the EFIR filter [1], [27], [30] is exploited as the auxiliary filter. This filter does not require the initial state and ignores the noise statistics that suit the requirements for an auxiliary filter that operates occasionally. The EFIR filter is based on the Taylor approximation, which requires computation of Jacobian matrices defined as

$$\mathbf{F}_k \triangleq \left.\frac{\partial \mathbf{f}_k}{\partial \mathbf{x}}\right|_{\hat{\mathbf{x}}_k}, \quad \mathbf{H}_k \triangleq \left.\frac{\partial \mathbf{h}_k}{\partial \mathbf{x}}\right|_{\hat{\mathbf{x}}_k}. \tag{10}$$

The EFIR filter equations for computing the state estimate and the estimation error covariance at time k are presented in Algorithm 2.

Algorithm 2. EFIR Filter

Data: M
Result: $\hat{\mathbf{x}}_k$, P_k
begin
- $t = k - M + 1$, $s = t + p - 1$.
- $\tilde{\mathbf{x}}_s = \hat{\mathbf{x}}_s$.
- $\tilde{\mathbf{P}}_s = \mathbf{P}_s$.
- $\mathcal{H}_{s,t} = \begin{bmatrix} \mathbf{H}_{t+2}\mathbf{F}_{t+2}\mathbf{F}_{t+1} \\ \mathbf{H}_{t+1}\mathbf{F}_{t+1} \\ \mathbf{H}_t \end{bmatrix}$.
- $\mathcal{F}_{s,0}^{t+1} = \mathbf{F}_s\mathbf{F}_{s-1}\cdots\mathbf{F}_{t+1}$.
- $\mathbf{G}_s = \mathcal{F}_{s,0}^{t+1}(\mathcal{H}_{s,t}^T\mathcal{H}_{s,t})^{-1}(\mathcal{F}_{s,0}^{t+1})^T$.
- **for** $l = s+1 : k$ **do**
  - $\tilde{\mathbf{x}}_l^- = \mathbf{f}_l(\tilde{\mathbf{x}}_{l-1}, \mathbf{u}_l)$.
  - $\tilde{\mathbf{P}}_l^- = \mathbf{F}_l\tilde{\mathbf{P}}_{l-1}\mathbf{F}_l^T + \mathbf{Q}_l$.
  - $\mathbf{G}_l = [\mathbf{H}_l^T\mathbf{H}_l + (\mathbf{F}_l\mathbf{G}_{l-1}\mathbf{F}_l^T)^{-1}]^{-1}$.
  - $\mathbf{K}_l = \mathbf{G}_l\mathbf{H}_l^T$.
  - $\tilde{\mathbf{x}}_l = \tilde{\mathbf{x}}_l^- + \mathbf{K}_l[\mathbf{z}_l - \mathbf{h}_l(\tilde{\mathbf{x}}_l^-)]$.
  - $\tilde{\mathbf{P}}_l = (\mathbf{I} - \mathbf{K}_l\mathbf{H}_l)\tilde{\mathbf{P}}_l^-(\mathbf{I} - \mathbf{K}_l\mathbf{H}_l)^T + \mathbf{K}_l\mathbf{R}_l\mathbf{K}_l^T$.
- **end for**
- $\hat{\mathbf{x}}_k = \tilde{\mathbf{x}}_k, \mathbf{P}_k = \tilde{\mathbf{P}}_k$.

end
† M is the horizon size of the EFIR filter.
† p is the dimension of the state vector.
† $\hat{\mathbf{x}}_s$ and $\mathbf{P}_s$ are the estimated state and the estimation error covariance, respectively, at time s, which can be obtained by using the extended minimum variance FIR (EMVF) filter [34].

In Algorithm 2, the EFIR filter is aided by the EMVF filter [34]. The EFIR filter is initialized by setting $\hat{\mathbf{x}}_s$ and $\mathbf{P_s}$, which can be obtained from other nonlinear filters (e.g., EKF) [1], [30]. As the EFIR filter is operated occasionally in the proposed hybrid RP/EFIR filtering, the EKF is not appropriate for the purpose of initialization. The EKF cannot be occasionally operated in the same manner with the EFIR filter, because the EKF requires $\hat{\mathbf{x}}_{k-1}$ for producing $\hat{\mathbf{x}}_k$. Thus, the EMVF filter, which can be operated in the same manner with the EFIR filter, is used to initialize the EFIR filter. The EMVF filter requires auxiliary signals $\tilde{\mathbf{z}}_k$ and $\tilde{\mathbf{u}}_k$, which are defined, respectively, as

$$\begin{aligned} \tilde{\mathbf{z}}_k &\triangleq \mathbf{h}_k(\hat{\mathbf{x}}_k) - \mathbf{H}_k\hat{\mathbf{x}}_k \\ \tilde{\mathbf{u}}_k &\triangleq \mathbf{f}_k(\hat{\mathbf{x}}_k) - \mathbf{F}_k\hat{\mathbf{x}}_k. \end{aligned} \tag{11}$$

Algorithm 3. EMVF Filter

Data: M
Result: $\hat{\mathbf{x}}_k$, $\mathbf{P}_k$
begin
- Obtain the state estimate, $\tilde{\mathbf{x}}_k$, using the following equations:
- $\tilde{\mathbf{x}}_k = \mathbf{L}(\mathbf{Y} - \overline{\mathbf{G}}\mathbf{U}) + \mathbf{K}\mathbf{U}$,
- $\mathbf{L} = \mathbf{J}\begin{bmatrix} \mathbf{W}_{1,1} & \mathbf{W}_{1,2} \\ \mathbf{W}_{1,2}^T & \mathbf{W}_{2,2} \end{bmatrix}^{-1}\begin{bmatrix} \overline{\mathbf{H}}^T \\ \overline{\mathbf{G}}^T \end{bmatrix}\overline{\mathbf{R}}^{-1}$,
- $\mathbf{J} = [\tilde{\mathcal{F}}_{n,m}\ \tilde{\mathcal{F}}_{n,m+1}\ \tilde{\mathcal{F}}_{n,m+2}\cdots\tilde{\mathcal{F}}_{n,n}I]$,
- $\tilde{\mathcal{F}}_{g,h} = \mathbf{F}_g \times \mathbf{F}_{g-1} \times \mathbf{F}_{g-2} \times \cdots \times \mathbf{F}_h\ (g \geq h)$,
- $\tilde{\mathcal{F}}_{g,g} = \mathbf{F}_g$,
- $\mathbf{W}_{1,1} = \overline{\mathbf{H}}^T\overline{\mathbf{R}}^{-1}\overline{\mathbf{H}}$,
- $\mathbf{W}_{1,2} = \overline{\mathbf{H}}^T\overline{\mathbf{R}}^{-1}\overline{\mathbf{G}}$,
- $\mathbf{W}_{2,2} = \overline{\mathbf{G}}^T\overline{\mathbf{R}}^{-1}\overline{\mathbf{G}} + \overline{\mathbf{Q}}^{-1}$,
- $\overline{\mathbf{H}} = \begin{bmatrix} \mathbf{H}_m \\ \mathbf{H}_{m+1}\tilde{\mathcal{F}}_{m,m} \\ \mathbf{H}_{m+2}\tilde{\mathcal{F}}_{m+1,m} \\ \vdots \\ \mathbf{H}_n\tilde{\mathcal{F}}_{n-1,m} \end{bmatrix}$,
- $\overline{\mathbf{G}} = \begin{bmatrix} \mathbf{0} & \mathbf{0} & \dots & \mathbf{0} & \mathbf{0} \\ \mathbf{H}_{m+1} & \mathbf{0} & \dots & \mathbf{0} & \mathbf{0} \\ \tilde{\mathcal{H}}_{m+2,m+1} & \mathbf{H}_{m+2} & \dots & \mathbf{0} & \mathbf{0} \\ \vdots & \vdots & \vdots & \vdots & \vdots \\ \tilde{\mathcal{H}}_{n,m+1} & \tilde{\mathcal{H}}_{n,m+2} & \dots & \tilde{\mathcal{H}}_n & \mathbf{0} \end{bmatrix}$,
- $\tilde{\mathcal{H}}_{g,h} = \mathbf{H}_g\tilde{\mathcal{F}}_{g-1,h}\ (g > h)$,
- $\overline{\mathbf{R}} = \left[\mathrm{diag}(\overbrace{\mathbf{R}_m\ \mathbf{R}_{m+1}\cdots\mathbf{R}_n}^{p})\right]$,
- $\overline{\mathbf{Q}} = \left[\mathrm{diag}(\overbrace{\mathbf{Q}_m\ \mathbf{Q}_{m+1}\cdots\mathbf{Q}_n}^{p})\right]$,
- $\mathbf{Y} = [\tilde{\mathbf{z}}_m^T\ \tilde{\mathbf{z}}_{m+1}^T\cdots\tilde{\mathbf{z}}_n^T]^T$,
- $\mathbf{U} = [\tilde{\mathbf{u}}_m^T\ \tilde{\mathbf{u}}_{m+1}^T\cdots\tilde{\mathbf{u}}_n^T]^T$,
- $\mathbf{K} = [\tilde{\mathcal{F}}_{n,m+1}\ \tilde{\mathcal{F}}_{n,m+2}\cdots\tilde{\mathcal{F}}_{n,n}\ I]$.
- Obtain the estimation error covariance, $\mathbf{P}_k$, using the following equation:
- $\mathbf{P}_k = \mathbf{K}\overline{\mathbf{Q}}\mathbf{K}^T + \mathbf{L}\overline{\mathbf{R}}\mathbf{L}^T$

end
† $m = k - M$ and $n = m + p - 1$ are the initial and final points, respectively, on the horizon of the EMVF filter.

The EMVF filter equations to obtain $\hat{\mathbf{x}}_k$ and $\mathbf{P}_k$ are presented in Algorithm 3. Substituting s into k in Algorithm 3, $\hat{\mathbf{x}}_s$ and $\mathbf{P}_s$ can be obtained. Note that the horizon size (i.e., averaging interval) of the EMVF filter is set to be the same as p, which is the dimension of the state vector and is the minimum available horizon size. The EMVF filter produces $\hat{\mathbf{x}}_s$ and $\mathbf{P}_s$ using the measurements on the interval $[k-M, k-M+p-1]$, and the EFIR filter updates them and produces $\hat{\mathbf{x}}_k$ and $\mathbf{P}_k$ using the measurements on the interval $[k-M+p, k]$.

Remark 1: The horizon size M is a key design parameter affecting the estimation performance of FIR filters [29], [34]. To achieve the best performance using FIR filters, M should be chosen to be an optimal horizon size. In nonlinear FIR filtering, such as the EFIR and the EMVF filtering, nonlinear system models are converted into linear time-varying (LTV) system models by means of the Taylor approximation. Thus, the optimal horizon size M_{opt} is also time-varying, which means M_{opt} should be found at each time step in nonlinear FIR filtering. Finding time-varying M_{opt} is a challenging problem in nonlinear FIR filtering. However, in the hybrid particle/FIR filtering, users do not need to worry about finding M_{opt}. This is because the nonlinear FIR filter is an auxiliary filter that is used to recover a failed PF. The recovery process by the nonlinear FIR filtering is performed very occasionally. For the most part of filtering time, the main filter (i.e., PF) produces state estimates. When the main filter fails, the auxiliary FIR filter provides a rough estimate of the current state. Using this information, the PF is reset and rebooted. Over time, the rough estimate of state obtained from the FIR filter is refined by the particle filtering. The nonlinear FIR filter is used to produce a rough estimate of state for resetting of the PF. Therefore, there is no need to find M_{opt} in the hybrid particle/FIR filtering. A roughly selected M is enough for the hybrid particle/FIR filtering. A small horizon size is advantageous for fast computation or real-time processing. However, the minimum horizon size, which is the same as the dimension of the state vector, may exhibit poor estimation performance owing to insufficient noise suppression. Thus, it is better to set the horizon size to be a slightly larger than the minimum available horizon size. Accordingly, in this paper, the horizon size was taken as $M = 5$, which is slightly larger than the minimum available horizon size $M = 4$.

C. Hybrid RP/EFIR Filter

The proposed hybrid particle/FIR filtering is a general algorithm that can adopt various particle and FIR filters. In this paper, an example of possible hybrid particle/FIR filters is presented. Combining the RPF [14], [19], [20] and the EFIR filter (Algorithm 2), the hybrid RP/EFIR filter is obtained. The choice of the RPF is due to its better robustness against sample impoverishment compared to the standard PF. Moreover, the performance of the RPF has been verified by a variety of applications. The algorithm of the RPF can be found in many studies [14], [19], [20]. In turn, the EFIR filter [1], [27], [30] is a state-of-the-art nonlinear iterative unbiased FIR filter having computational efficiency. The hybrid RP/EFIR filtering (Algorithm 4) follows the procedure shown in Fig. 3.

Algorithm 4. Hybrid RP/EFIR Filter

Data: N, M, χ^2
Result: $\hat{\mathbf{x}}_k$
begin
  - Generate N initial particles.
  for $k = 1, 2, \cdots$ **do**
    - Perform filtering using the RPF and obtain the *a posteriori* particle set $\{\hat{\mathbf{x}}^+_{k,i}\}_{i=1}^N$.
    - $\hat{\mathbf{x}}_k = \hat{\mathbf{x}}_{k,\text{RPF}} = \frac{1}{N}\sum_{i=1}^N \hat{\mathbf{x}}^+_{k,i}$.
    - Compute the Jacobian matrices $\mathbf{F}_k$ and $\mathbf{H}_k$ defined in (10), and save them in the memory.
    - Compute the auxiliary signals $\tilde{\mathbf{z}}_k$ and $\tilde{\mathbf{u}}_k$ defined in (11), and save them in the memory.
    if $k > M$ **then**
      - Diagnose the RPF failure by using Algorithm 1.
      if $I_{\text{failure}} == 1$ **then**
        - $s = t + p - 1$.
        - For initialization of the EFIR filter, execute the EMVF filter (Algorithm 3) and obtain $\hat{\mathbf{x}}_s$ and $\mathbf{P}_s$.
        - Perform filtering using the EFIR filter (Algorithm 2) and obtain $\hat{\mathbf{x}}_{k,\text{EFIR}}$ and $\mathbf{P}_{k,\text{EFIR}}$.
        - $\hat{\mathbf{x}}_k = \hat{\mathbf{x}}_{k,\text{EFIR}}$.
        - Reset the RPF by generating new *a posteriori* particles using Gaussian distribution: $\hat{\mathbf{x}}^+_{k,i} \sim \mathcal{N}(\hat{\mathbf{x}}_{k,\text{EFIR}}, \mathbf{P}_{k,\text{EFIR}})$.
      end if
    end if
  end for
end
† $\hat{\mathbf{x}}_{k,\text{EFIR}}$ and $\mathbf{P}_{k,\text{EFIR}}$ are the estimated state and the estimation error covariance obtained using the EFIR filter.
† $\hat{\mathbf{x}}_{k,\text{RPF}}$ is the estimated state obtained by using the RPF.
† $\hat{\mathbf{x}}_k$ is the output of the hybrid RP/EFIR filter.

In Algorithm 4, the Gaussian kernel [14], [19] is used for the regularization process of the RPF. The optimal bandwidth of the Gaussian kernel is computed as

$$h_{\text{opt}} = [4/(p+2)]^{\frac{1}{p+4}} N^{-\frac{1}{p+4}} \tag{12}$$

where p is the dimension of the state vector [19]. Algorithm 4 is computationally efficient, because the EFIR filter operates on short horizons and only by request. Unlike the existing versions of PFs [16], [20]–[22], which were designed to alleviate sample impoverishment, Algorithm 4 provides recovery of the RPF when the RPF failures occur.

IV. Mobile Robot Localization Using WSN via Hybrid Particle/FIR Filtering

In this section, the designed hybrid RP/EFIR filter is applied to the mobile robot localization using a WSN. Various conditions that may cause the RPF to fail are considered.

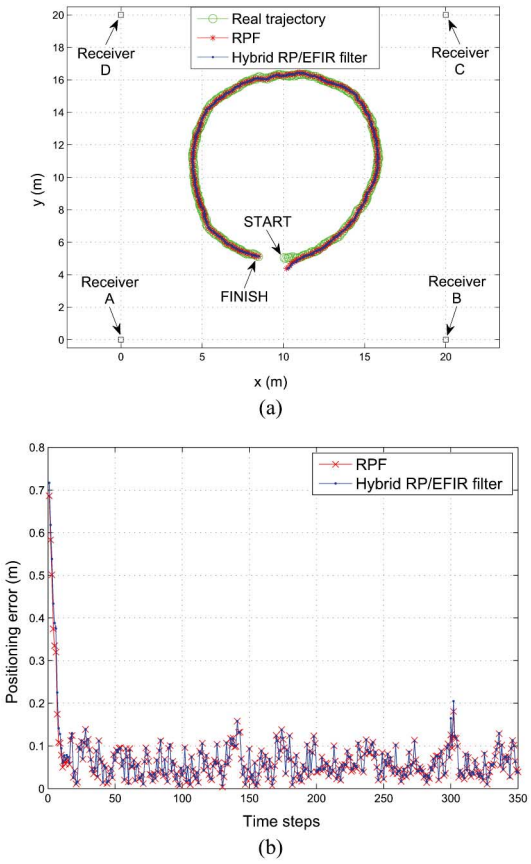

Fig. 4. Mobile robot localization under the ideal conditions of no sample impoverishment. (a) Robot trajectory. (b) Instantaneous positioning errors.

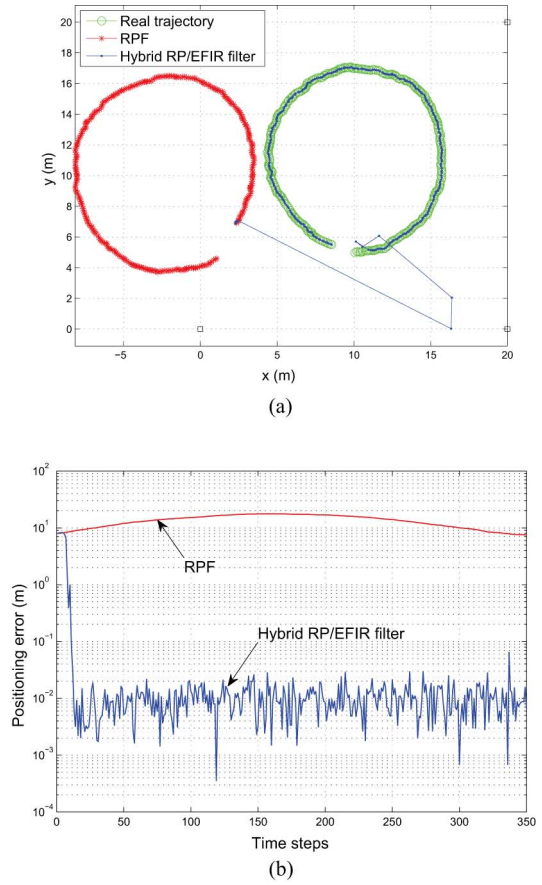

Fig. 5. Mobile robot localization with small measurement noise. (a) Actual robot trajectory and its estimates. (b) Instantaneous positioning errors.

Four receivers (Fig. 1) are assumed to be installed at points $(0,0)$, $(0,20)$, $(20,0)$, and $(20,20)$, all in meters. In all subsequent simulations, the horizon size of the EFIR filter is taken as $M=5$.

A. Circular Robot Trajectory

First, the proposed hybrid RP/EFIR filter is tested under ideal conditions (i.e., when sample impoverishment is negligible and localization is thus provided with highest accuracy). A robot departs from point (10 and 5 m) and travels counterclockwise along a circular trajectory. The noise covariances are set as $\mathbf{Q}_k = [\text{diag}(0.1^2\ 0.1^2\ 1^2)]$ and $\mathbf{R}_k = [\text{diag}(0.5^2\ 0.5^2\ 0.5^2\ 1^2)]$. The generated number of particles is $N = 10^4$. The positioning error is computed by

$$E_{\text{pos}} = \sqrt{(x_k - \hat{x}_k)^2 + (y_k - \hat{y}_k)^2} \tag{13}$$

where (x_k, y_k) is the true position of a mobile robot and $(\hat{x}_k, \hat{y}_k)$ is its estimated position. Fig. 4(a) shows how well the estimated location fits an actual trajectory. In Fig. 4(b), the same errors are observed in the RPF and the hybrid RP/EFIR filter, as would be expected with no sample impoverishment. Note that the auxiliary EFIR filter stays out of service here and the hybrid RP/EFIR filter operates as a pure RPF.

1) Localization With Small Measurement Noise: In robot localization, sample impoverishment typically occurs when a sensor is accurate and measurement noise is small. A curiosity of this situation is that an increase in sensing accuracy causes more frequent localization failures [18]. Under this condition of low measurement noise caused by very accurate measurement of the WSN, the hybrid RP/EFIR filter is tested. The measurement noise covariance is taken as $\mathbf{R}_k = [\text{diag}(0.05^2\ 0.05^2\ 0.05^2\ 0.1^2)]$. Fig. 5 sketches the localization errors. As can be seen in Fig. 5(a), the RPF completely fails in tracking across all points due to sample impoverishment. Even though the RPF is more robust than the standard PF, it was unable to avoid sample impoverishment entirely with small measurement noise. On the contrary, the hybrid RP/EFIR filter does this work perfectly, and Fig. 5(b) shows extremely low positioning errors.

2) Localization with Small Number of Particles: A small number of particles is always desirable from the standpoint of fast (real-time) filtering. This requirement typically cannot be obeyed because it leads to poor performance and PF failures. A large number of particles (e.g., $N = 10\,000$) are commonly generated.

Fig. 6 sketches a typical effect associated with a small number of particles ($N = 1000$). As can be seen, the RPF has a transient region lasting up to $k = 30$ in this case. This can be explained in the following way. As suggested by the optimization theory for an unknown initial target's position, the particles are commonly generated to have a uniform distribution. This

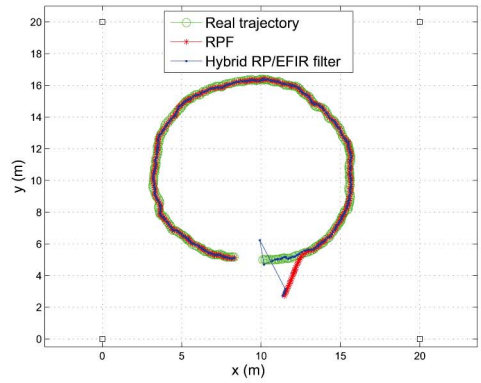

(a)

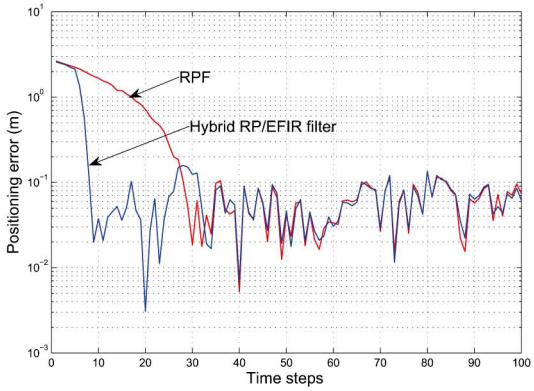

(b)

Fig. 6. Mobile robot localization with a small number of the particles ($N = 1000$). (a) Actual and estimated trajectories. (b) Positioning errors.

should be so for infinity N. Otherwise, if N is finite, the distribution histogram is not uniform and particles are concentrated in certain areas. This biased estimate of the initial state causes localization errors. In the RPF scheme, the bias error typically diminishes during a long transience. The EFIR filter is unbiased and its estimate is produced on a short horizon $M = 5$, which is statistically more accurate than that obtained for PF with small N. Therefore, in contrast, transients in the RP/EFIR filter appear to be much shorter [Fig. 6(b)].

Fig. 7 gives typical average localization errors produced by the RPF and the hybrid RP/EFIR filter for $1000 \leqslant N \leqslant 5000$. The hybrid RP/EFIR filter is more successful in terms of accuracy than the RPF, and the error difference between these filters vanishes as N increases. Note that $N > 10^4$ makes errors in both filters almost equal.

The effect of N on the positioning errors is much more pronounced when the number of generated particles is very small (e.g., $N < 500$). Fig. 8 gives the number of failures detected in the RPF and the hybrid RP/EFIR filter in 100 Monte Carlo runs. An estimator was deemed to fail (i.e., localization failure) if an average positioning error exceeded 1m. As can be seen, an unacceptably large number of failures is produced by the RPF with $N = 100$ and the number of failures decreases when N grows. On the contrary, one failure was not detected with the hybrid RP/EFIR filter.

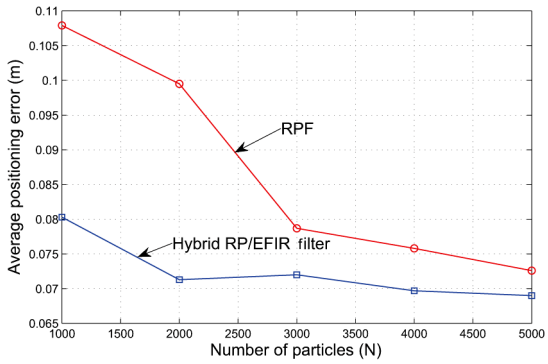

Fig. 7. Typical average positioning errors as functions of the number N of the particles for RPF and hybrid RP/EFIR filter.

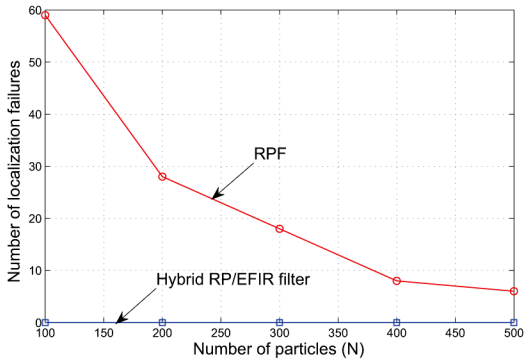

Fig. 8. Localization failures detected in the RPF and hybrid RP/EFIR filter with very small N values.

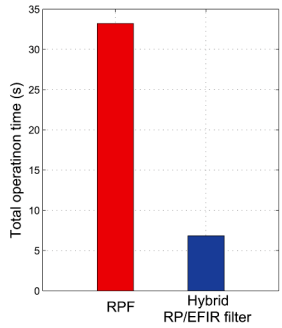

Fig. 9. Example of the computation time consumed by the RPF and hybrid RP/EFIR filter to localize a robot with an error of 10 cm.

Operated on short horizons (e.g., $M = 5$), an auxiliary EFIR filer does not consume much extra time, so for $N = 10^4$, the total operation time measured was 155.12 s in the RPF and 155.47 s in RP/EFIR filter. A dramatic reduction in computation time is indicated if measuring it for the same positioning error, as shown in Fig. 9. The two bars represent the total time consumed by the RPF and hybrid RP/EFIR filter to localize a mobile robot with an error of 10 cm. More specifically, the RPF required 33.22 s to provide a localization with an error of 9.5 cm for $N = 2000$. In turn, the hybrid RP/EFIR filter required 6.84 s to provide a localization with an error of 8.9 cm for $N = 400$.

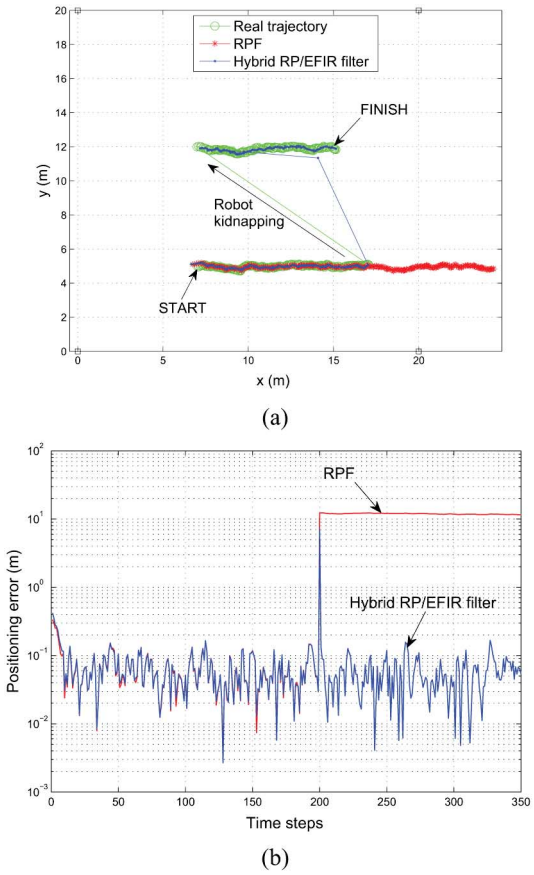

Fig. 10. "Kidnapped robot problem." (a) Mobile robot trajectory and its estimates. (b) Positioning errors.

B. Kidnapped Robot Problem

The kidnapped robot problem is one of the most challenging in mobile robot localization. It requires that the localization algorithm has an ability to recover from extreme failures [16]. Below, the RPF and hybrid RP/EFIR filter are tested by the kidnapped robot problem. The simulation scenario is as follows.

1) A mobile robot starts from point (7 and 5 m) and travels along a straight line.
2) At the 200th step, the robot suddenly "jumps" (is kidnapped) to (7 and 12 m).
3) Thereafter, it keeps traveling along the straight line in the same direction.

This scenario is somewhat artificial as long as sudden jumps are unfeasible in robotics. Even so, it allows localization algorithm testing under unpredictable behaviors such as the "kidnapped robot problem." Fig. 10 gives an idea about tracking abilities of both filters before and after the breakpoint of the "kidnapping." As can be seen, the RPF completely loses any ability for tracking at the breakpoint, whereas the RP/EFIR filter still tracks a robot after a short period of transience. This simulation also speaks in favor of the proposed hybrid filter.

V. Conclusion

The hybrid particle/FIR filtering algorithm proposed in this paper has demonstrated the ability to recover a completely failed PF algorithm. This effect was achieved by the PF resetting using an auxiliary FIR filter that has special robustness and stability. Simulation results and statistical analyses demonstrated that the hybrid RP/EFIR filter improves reliability of localization compared to the RPF. Under harsh conditions, such as low measurement noise or a small number of particles, the hybrid RP/EFIR filter did not fail and was successful in tracking the robot position, whereas the RPF exhibited large positioning errors or completely failed localization results. In addition, the hybrid RP/EFIR filter reached the required localization accuracy with a much smaller number of particles compared to the RPF. Thus, the proposed hybrid filter structure can offer a dramatic reduction in computation time.

The greatest advantage of the proposed algorithm is that it can adopt any PF and any FIR filter. By combining state-of-the-art filters, an upgraded hybrid particle/FIR filter can be made. The present authors are now developing and testing a new FIR filter that can overcome the intermittent measurement condition. Using the new FIR filter, a new hybrid particle/FIR filter for overcoming the NLOS situation will be made. In addition, we plan to experiment the indoor mobile robot localization using the proposed algorithm. The results of those studies are expected to be published in the near future.

References

[1] J. Pomarico-Franquiz and Y. S. Shmaliy, "Accurate self-localization in RFID tag information grids using FIR filtering," *IEEE Trans. Ind. Informat.*, vol. 10, no. 2, pp. 1317–1326, May 2014.
[2] J. Rodriguez-Araujo, J. J. Rodriguez-Andina, J. Farina, and M. Y. Chow, "Field-programmable system-on-chip for localization of UGVs in an indoor ispace," *IEEE Trans. Ind. Informat.*, vol. 10, no. 2, pp. 1033–1043, May 2014.
[3] K. Derr and M. Manic, "Wireless sensor networks–node localization for various industry problems," *IEEE Trans. Ind. Informat.*, vol. 11, no. 3, pp. 752–762, Jun. 2015.
[4] D. Zhang, S. Zhao, L. T. Yang, M. Chen, Y. Wang, and H. Liu, "NextMe: Localization using cellular traces in internet of things," *IEEE Trans. Ind. Informat.*, vol. 11, no. 2, pp. 302–312, Apr. 2015.
[5] A. C. Paredes, M. Malfaz, and M. A. Salichs, "Signage system for the navigation of autonomous robots in indoor environments," *IEEE Trans. Ind. Informat.*, vol. 10, no. 1, pp. 680–688, Feb. 2014.
[6] A. Abu-Mahfouz and G. P. Hancke, "Distance bounding: A practical security solution for real-time location systems," *IEEE Trans. Ind. Informat.*, vol. 9, no. 1, pp. 16–27, Feb. 2013.
[7] Y. Toda and N. Kubota, "Self-localization based on multiresolution map for remote control of multiple mobile robots," *IEEE Trans. Ind. Informat.*, vol. 9, no. 3, pp. 1772–1781, Aug. 2013.
[8] J. Park and J. Lee, "A beacon color code scheduling for the localization of multiple robots," *IEEE Trans. Ind. Informat.*, vol. 7, no. 3, pp. 467–475, Aug. 2011.
[9] H. Liu, H. Darabi, P. Banerjee, and J. Liu, "Survey of wireless indoor positioning technique and systems," *IEEE Trans. Syst. Man Cybern.*, vol. 37, no. 6, pp. 1067–1080, Nov. 2007.
[10] P. Yang and W. Wu, "Efficient particle filter localization algorithm in dense passive RFID tag environment," *IEEE Trans. Ind. Electron.*, vol. 61, no. 10, pp. 5641–5651, Oct. 2014.
[11] J. Wang, Q. Gao, Y. Yu, H. Wang, and M. Jin, "Toward robust indoor localization based on Bayesian filter using chirp-spread-spectrum ranging," *IEEE Trans. Ind. Electron.*, vol. 59, no. 3, pp. 1622–1629, Mar. 2012.
[12] J. M. Huerta, J. Vidal, A. Giremus, and J. Tourneret, "Joint particle filter and UKF position tracking in severe non-line-of-sight situations," *IEEE J. Sel. Topics Signal Process.*, vol. 3, no. 5, pp. 874–888, Oct. 2009.
[13] C. K. Ahn, P. Shi, and M. V. Basin, "Two-dimensional dissipative control and filtering for Roesser model," *IEEE Trans. Autom. Control*, vol. 60, no. 7, pp. 1745–1759, Jul. 2015.

[14] D. Simon, Optimal State Estimation: Kalman, H_∞, and Nonlinear Approaches. Hoboken, NJ, USA: Wiley, 2006.
[15] J. Gonzalez *et al.*, "Mobile robot localization based on ultra-wide-band ranging: A particle filter approach," *Robot. Auton. Syst.*, vol. 57, no. 5, pp. 496–507, May 2009.
[16] S. Thrun, D. Fox, W. Burgard, and F. Dellaert, "Robust Monte Carlo localization for mobile robots," *Artif. Intell.*, vol. 128, no. 1–2, pp. 99–141, May 2000.
[17] D. Fox, W. Burgard, H. Kruppa, and S. Thrun, "Monte Calro localization: Efficient position estimation for mobile robots," in *Proc. Nat. Conf. Artif. Intell. (AAAI)*, 1999, pp. 343–349.
[18] S. Thrun, W. Burgard, and D. Fox, *Probabilistic Robotics*. Cambridge, MA, USA: MIT Press, 2005.
[19] B. Ristic, S. Arulampalam, and N. Gordon, *Beyond the Kalman Filter: Particle Filters for Tracking Applications*. Norwood, MA, USA: Arctech House, 2004.
[20] N. Oudjane and C. Musso, "Progressive correction for regularized particle filters," in *Proc. 3rd Int. Conf. Inf. Fusion*, Paris, France, 2000, vol. 2, pp. THB2/10–THB2/17.
[21] W. R. Gilks and C. Berzuini, "Following a moving target—Monte Carlo inference for dynamic Bayesian models," *J. Roy. Stat. Soc. B (Stat. Methodol.)*, vol. 63, no. 1, pp. 127–146, 2001.
[22] A. Doucet, S. Godsill, and C. Andrieu, "On sequential Monte Carlo sampling methods for Bayesian filtering," *Statist. Comput.*, vol. 10, no. 3, pp. 197–208, Jul. 2000.
[23] S. Lenser and M. Veloso, "Sensor resetting localization for poorly modelled mobile robots," in *Proc. Int. Conf. Robot. Autom. (ICRA)*, 2000, pp. 1225–1232.
[24] Y. S. Shmaliy, "Unbiased FIR filtering of discrete-time polynomial state-space models," *IEEE Trans. Signal Process.*, vol. 57, no. 4, pp. 1241–1249, Apr. 2009.
[25] Y. S. Shmaliy, "Linear optimal FIR estimation of discrete time-invariant state-space models," *IEEE Trans. Signal Process.*, vol. 58, no. 6, pp. 3086–3096, Jun. 2010.
[26] Y. S. Shmaliy, "An iterative Kalman-like algorithm ignoring noise and initial conditions," *IEEE Trans. Signal Process.*, vol. 59, no. 6, pp. 2465–2473, Jun. 2011.
[27] Y. S. Shmaliy, "Suboptimal FIR filtering of nonlinear models in additive white Gaussian noise," *IEEE Trans. Signal Process.*, vol. 60, no. 10, pp. 5519–5527, Oct. 2012.
[28] D. Simon and Y. S. Shmaliy, "Unified forms for Kalman and finite impulse response filtering and smoothing," *Automatica*, vol. 49, no. 6, pp. 1892–1899, Jun. 2013.
[29] F. Ramirez-Echeverria, A. Sarr, and Y. S. Shmaliy, "Optimal memory of discrete-time FIR filters in state-space," *IEEE Trans. Signal Process.*, vol. 62, no. 3, pp. 557–561, Feb. 2014.
[30] J. Pomarico-Franquiz, S. H. Khan, and Y. S. Shmaliy, "Combined extended FIR/Kalman filtering for indoor robot localization via triangulation," *Measurement*, vol. 50, pp. 236–243, Apr. 2014.
[31] C. K. Ahn, S. Han, and W. H. Kwon, "H_∞ FIR filters for linear continuous-time state-space systems," *IEEE Signal Process. Lett.*, vol. 13, no. 9, pp. 557–560, Sep. 2006.
[32] C. K. Ahn, "Strictly passive FIR filtering for state-space models with external disturbance," *Int. J. Electron. Commun.*, vol. 66, no. 11, pp. 944–948, Nov. 2012.
[33] C. K. Ahn, "A new solution to the induced l_∞ finite impulse response filtering problem based on two matrix inequalities," *Int. J. Control*, vol. 87, no. 2, pp. 404–409, 2014.
[34] J. M. Pak, C. K. Ahn, M. T. Lim, and M. K. Song, "Horizon group shift FIR filter: Alternative nonlinear filter using finite recent measurements," *Measurement*, vol. 57, pp. 33–45, Nov. 2014.
[35] I. H. Choi, J. M. Pak, C. K. Ahn, Y. H. Mo, M. T. Lim, and M. K. Song, "New preceding vehicle tracking algorithm based on optimal unbiased finite memory filter," *Measurement*, vol. 73, pp. 262–274, Sep. 2015.
[36] G. Campion, G. Bastin, and B. D'Andrea-Novel, "Structural properties and classification of kinematic and dynamic models of wheeled mobile robots," *IEEE Trans. Robot. Autom.*, vol. 12, no. 1, pp. 47–62, Feb. 1996.
[37] K. Komoriya and E. Oyama, "Position estimation of a mobile robot using optical fiber gyroscope," in *Proc. IEEE/RSJ/GI Int. Conf. Intell. Robots Syst.*, 1994, vol. 1, pp. 143–149.
[38] S. K. Singh, M. Premalatha, and G. Nair, "Ellipsoidal gating for an airborne track while scan radar," in *Proc. IEEE Int. Radar Conf.*, May 1995, pp. 334–339.
[39] P. C. Mahalanobis, "On the generalised distance in statistics," in *Proc. Nat. Inst. Sci.*, Calcutta, India, Apr. 1936.
[40] R. C. Smith and P. Cheeseman, "On the representation and estimation of spatial uncertainty," *Int. J. Robot. Res.*, vol. 5, no. 4, pp. 56–68, Winter 1986.

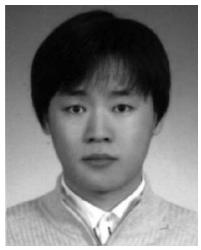

Jung Min Pak received the B.S., M.S., and Ph.D. degrees in electrical engineering from Korea University, Seoul, Korea, in 2006, 2008, and 2015, respectively.

Since 2015, he has been a Postdoctoral Researcher with the School of Electrical Engineering, Korea University. His research interests include finite impulse response filter, particle filter, mobile robot localization, and visual object tracking.

Choon Ki Ahn (M'06–SM'12) received the B.S. and M.S. degrees in electrical engineering from Korea University, Seoul, Korea, in 2000 and 2002, respectively, and the Ph.D. degree in electrical engineering and computer science from Seoul National University, Seoul, Korea, in 2006.

He is currently a Professor with the School of Electrical Engineering, Korea University. His research interests are finite impulse response filtering, two-dimensional systems, and intelligent systems.

Dr. Ahn has been on the Editorial Board of the *Journal of the Franklin Institute*; the *International Journal of Control, Automation, and Systems; Mathematical Problems in Engineering*; the *Scientific World Journal*; *Scientific Research and Essays*; and the *Journal of the Institute of Control, Robotics, and Systems*. He was the recipient of the Medal for "Top 100 Engineers" 2010 by IBC, Cambridge, U.K. In 2012, his European Physical Journal E paper was ranked #1 in the TOP 20 Articles in the field of neural networks by BioMedLib.

Yuriy S. Shmaliy (M'96–SM'00–F'11) received the B.S., M.S., and Ph.D. degrees from the Kharkiv Aviation Institute, Kharkiv, Ukraine, in 1974, 1976 and 1982, respectively, all in electrical engineering, and the D.Sc. degree in electrical engineering from the Kharkiv Railroad Institute, Kharkiv, Ukraine, in 1992.

In 1986, he served as a Full Professor. From 1985 to 1999, he was with Kharkiv Military University. In 1992, he founded the Scientific Center "Sichron," Kharkiv, Ukraine, where he was the Director in 2002. Since 1999, he was a Professor with Universidad de Guanajuato of Mexico, Guanajuato, Mexico, and since 2012, the Head of the Department of Electronics Engineering. Currently, he is a Visiting Professor with City University London, London, U.K. He has published 365 journals and conference papers, and 81 patents. He is the author of several books: *Continuous-Time Signals* (Springer, 2006), *Continuous-Time Systems* (Springer, 2007), *GPS-Based Optimal FIR Filtering of Clock Models* (2009), and *Probability: Interpretation, Theory, and Applications* (Nova Science Publishing, 2012). His research interests include optimal estimation, statistical signal processing, and stochastic system theory.

Dr. Shmaliy is currently an Associate Editor and an Editorial Board Member for several journals. He was rewarded a title, Honorary Radio Engineer of the USSR, in 1991. He was the recipient of the Royal Academy of Engineering Newton Collaboration Program Award in 2015.

Myo Taeg Lim (M'94) received the B.S. and M.S. degrees from Korea University, Seoul, Korea, in 1985 and 1987, respectively, and the M.S. and Ph.D. degrees from Rutgers University, New Brunswick, NJ, USA, in 1990 and 1994, respectively, all in electrical engineering.

Since 1996, he has been a Professor with the School of Electrical Engineering, Korea University. He is the author or co-author of more that 60 journal papers and two books: *Optimal Control of Singularly Perturbed Linear Systems and Application: High-Accuracy Techniques* (Marcel Dekker, 2001) and *Optimal Control: Weakly Coupled Systems and Applications* (CRC Press, 2009). His research interests include optimal and robust control, vision based motion control, and autonomous mobile robots.

Dr. Lim is an Editor of the *International Journal of Control, Automation, and Systems* (IJCAS). He is a Fellow of the Institute of Control, Robotics, and Systems (ICROS).